Optics Communications 282 (2009) 3024–3027

Contents lists available at ScienceDirect

Optics Communications

journal homepage: www.elsevier.com/locate/optcom

Controlled observation of nondegenerate cavity modes in a microdroplet on a superhydrophobic surface

S.C. Yorulmaz [a], M. Mestre [a], M. Muradoglu [b], B.E. Alaca [b], A. Kiraz [a,*]

[a] Department of Physics, Koç University, Rumelifeneri Yolu, Sariyer, 34450 Istanbul, Turkey
[b] Department of Mechanical Engineering, Koç University, Rumelifeneri Yolu, Sariyer, 34450 Istanbul, Turkey

ARTICLE INFO

Article history:
Received 9 January 2009
Received in revised form 27 March 2009
Accepted 6 April 2009

ABSTRACT

We demonstrate controlled lifting of the azimuthal degeneracy of the whispering gallery modes (WGMs) of single glycerol–water microdroplets standing on a superhydrophobic surface by using a uniform electric field. A good agreement is observed between the measured spectral positions of the nondegenerate WGMs and predictions made for a prolate spheroid. Our results reveal fewer azimuthal modes than expected from an ideal spherical microdroplet due to the truncation by the surface. We use this difference to estimate the contact angles of the microdroplets.

1. Introduction

Liquid microdroplets are ideally suited for applications that benefit from the intriguing properties of the whispering gallery modes (WGMs) because of their spherical shapes, smooth surfaces, biocompatibility, and flexible nature [1]. For over 30 years, WGMs have been used in developing many microdroplet-based applications in quantum and nonlinear optics, aerosol science, and chemical physics [2]. We have recently demonstrated that the use of a superhydrophobic surface greatly facilitates such experiments, and brings together critical advantages over other techniques used in microdroplet stabilization [3]. In addition to preserving the sphericity of the microdroplet, the superhydrophobic surface increases the robustness of the experiments against external disturbances. Furthermore, this experimental configuration enables the integration of liquid microdroplets with other optoelectronic components. Measurements reported in this letter especially benefit from this advantage by combining microfabricated electrical contacts with microdroplets.

WGMs of an ideal sphere are identified by polarization (TE, TM), radial mode order n, angular momentum number l, and azimuthal mode number m ranging between $[-l, l]$. They are described by the vector spherical harmonics and spherical Bessel functions [4]. Glycerol–water microdroplets standing on a superhydrophobic surface take the shape of a truncated microsphere. WGM solutions of an ideal truncated dielectric sphere are similar to those of an ideal dielectric sphere. In particular, their spectral positions remain unchanged within the resolution used in our experiments [5]. For an ideal dielectric sphere, WGMs with the same polarization, radial mode order, and angular momentum number have $2l+1$ azimuthal degeneracy. The difference between the ideal and truncated cases should become apparent when the azimuthal degeneracy of the WGMs is lifted. The experiments reported in this letter rely on the deformation of microdroplets towards a prolate spheroid using a uniform electric field applied parallel to the superhydrophobic surface. Our results reveal fewer azimuthal modes than expected from an ideal spherical microdroplet. This is consistent with the truncation by a surface with a high refractive index that should prevent the propagation of the WGMs that cross the solid–liquid interface. We use this difference between the observed number of azimuthal modes and that expected from an ideal microsphere to estimate the contact angle. We note that degeneracy breaking of the WGMs has been previously demonstrated for liquid microdroplets [6,7], and solid microspheres [8–10]. Major differences of our demonstration from the previous ones include the controlled nature of the deformation mechanism for liquid microdroplets, and the use of the superhydrophobic surface.

An illustration of the experimental configuration is shown in Fig. 1. Photolithography with positive-tone resist was used for indium tin oxide (ITO) contact preparation. During the wet etching process, HCl was used to dissolve the ITO coating in the center, and obtain the pattern consisting of two contacts separated by around 35 μm. Samples were then spin coated with hydrophobically coated silica nanoparticles, revealing superhydrophobic surfaces that are transparent to visible light and contain a nanoscale surface, as reported previously [3]. Microdroplets with diameters ranging from a few up to ~20 μm were generated by an ultrasonic nebulizer using a glycerol–water solution with 10/90 volume fraction, containing 2 μM Rhodamine B dye molecules. Upon their generation, glycerol–water microdroplets quickly evaporate and reach their equilibrium sizes determined by the relative water humidity in the ambient atmosphere (measured to be $62 \pm 5\%$ in the experiments reported in this letter). The equilib-

* Corresponding author. Tel.: +90 212 3381701; fax: +90 212 3381559.
E-mail address: akiraz@ku.edu.tr (A. Kiraz).

0030-4018/$ - see front matter © 2009 Elsevier B.V. All rights reserved.
doi:10.1016/j.optcom.2009.04.016

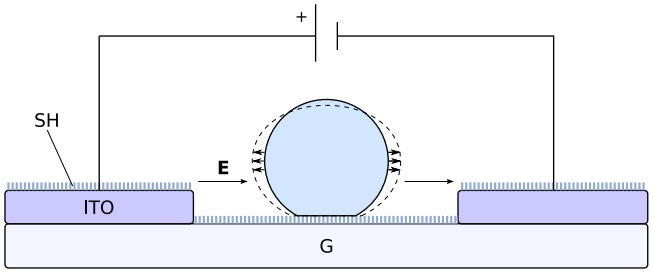

Fig. 1. Experimental setup (not to scale). G: cover glass; SH: superhydrophobic coating; ITO: indium tin oxide contacts. The dashed line shows the deformed microdroplet under the influence of the electric field.

rium volume fraction of glycerol to water was then 65/35 [11]. Optical experiments were performed within one day following microdroplet generation. Using microscope images we verified that the size reduction due to glycerol evaporation was barely observable during this one day period, in the absence of laser excitation. Our calculations also predict $< 1\%$ size reduction in these conditions [11]. In the optical setup, individual microdroplets were excited with a cw solid state green laser ($\lambda = 532$ nm) using a microscope objective (NA = 0.80, 60×) in the inverted geometry. Excitation powers used in the experiments were between 1 and 10 μW at the focus of the microscope objective. Fluorescence was collected with the same microscope objective, dispersed with a 50 cm monochromator (spectral resolution: 0.07 nm), and detected with a CCD camera using 1–3 s exposure times. Voltages up to ~450 V were used for electric field generation.

It is well known that an isolated liquid droplet is distorted into a prolate spheroid in the direction of a uniform electric field, when the deformation is small [12,13]. The deformation is usually defined as $D = (r_p - r_e)/(r_p + r_e)$ where r_p and r_e are the semimajor and semiminor axes of the spheroidal droplet parallel and perpendicular to the applied field, respectively. Deformation is in general a function of the resistivity, permittivity and viscosity ratios of the droplet to the surrounding air, and the electrical capillary number defined as $C_e = r_o \epsilon E^2/\gamma$ where r_o, ϵ, E and γ are the equivalent radius of the droplet, the permittivity of air, electric field strength far from the droplet, and surface tension coefficient, respectively. Since the conductivity of glycerol is much higher than that of air, the deformation of an isolated glycerol microdroplet in air can be approximated as $D = 9C_e/16$ [12,13].

For a microsphere that is slightly distorted towards a spheroid, the azimuthal degeneracy of the WGMs is lifted as [7]

$$\omega(m) = \omega_0\left[1 - \frac{e}{6}\left(1 - \frac{3m^2}{l(l+1)}\right)\right], \quad (1)$$

where ω_0 is the frequency of the degenerate WGM of the microsphere, and e is the distortion amplitude defined as $e = (r_p - r_e)/r_o$ ($e > 0$ and $e < 0$ for a prolate and oblate spheroid, respectively). For small deformations, D and e are related as $D \approx e/2$.

Fig. 2a shows consecutive normalized spectra recorded from a 5.2 μm diameter microdroplet as voltage applied between the contacts is first increased from 0 to 380 V, and then decreased back to 0 V. Photobleaching put a limit of ~50 on the total number of spectra that could be recorded from a microdroplet using the selected excitation intensity and dye concentration. This however did not influence the observed spectral patterns which are the subject of this study. The single peak observed in the first spectrum at 0 V corresponds to azimuthally degenerate WGMs with the same polarization, radial mode order, and angular momentum number. The fact that the line shape of this peak is well preserved in the dashed spectrum acquired when the voltage is decreased back to

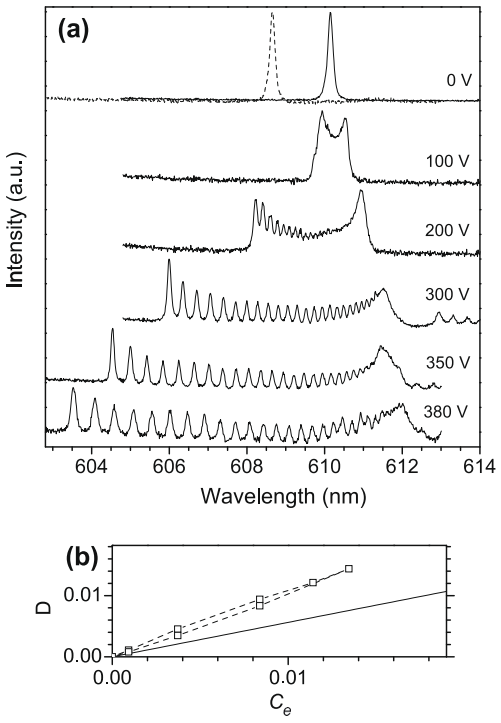

Fig. 2. (a) Successive spectra recorded from a 5.2 μm diameter microdroplet at different voltages. The dashed spectrum at 0 V was obtained after a full cycle of increasing and decreasing the voltage. (b) Electrical capillary number dependence of the deformation. The theoretical curve (solid line) and the experimental curve (dashed line with symbols) measured as the voltage is first increased from and decreased to zero are plotted.

0 V shows the controlled nature of the deformation scheme we present here. The slight blue shift of the dashed spectrum with respect to the solid spectrum corresponds to a reduction in the microdroplet size by 0.24%. This indicates the evaporation of glycerol during the period when consecutive spectra are recorded (a few minutes), caused mainly by laser heating. These evaporation levels still enable tracking of the specific WGM between consecutive spectra, hence allowing for the analysis of its degeneracy lifting. With the applied voltage, the azimuthal degeneracy between the WGMs is lifted, and well-resolved peaks are observed, especially in the low wavelength region of the spectrum. In agreement with a deformation towards a prolate spheroid, each peak is twofold degenerate ($+m, -m$), and the azimuthal mode numbers of the WGMs approach zero with increasing wavelengths. With an increase in $|m|$ (decrease in wavelength), spatial profiles of the WGMs approach the solid–liquid interface, m=0 corresponding to the WGM peaked on the equatorial plane and parallel to the surface. In Fig. 2a, for a high voltage spectrum, an increase is observed in the relative intensity of the peaks at lower wavelengths. This is explained by the excitation of the microdroplets near their centers in our experiments. These excitation conditions allow for a clear determination of the lowest wavelength peak which is critical in the contact angle estimation.

In Fig. 2b we also plot the change in the deformation D as a function of the electrical capillary number C_e. Deformation is determined by the spectral spacing between the WGM with m=0 (located approximately at the middle point of the highest wavelength hill in the spectrum) and that having the highest $|m|$ using $\Delta\lambda/\lambda_0 \approx -D$, obtained from Eq. (1) for large l. Two dimensional electrostatics simulations (performed with COMSOL®) are used in estimating the electrical capillary numbers, considering the surface tension coefficient of the binary microdroplet in our experimental conditions ($\gamma = 0.0677$ N/m [14]). Our experiments reveal an al-

most linear relationship between D and C_e, in agreement with the theoretical prediction. The difference between the theoretical and experimental slopes in Fig. 2b is attributed to the presence of the superhydrophobic surface and a slight nonuniformity of the electric field.

Detailed analyses of the relative locations of the peaks obtained upon the lifting of the degeneracy are presented in Fig. 3 for the microdroplet discussed in Fig. 2 (microdroplet 1) and another 5.0 μm diameter microdroplet (microdroplet 2). For a given spectrum we first identify the peak locations. Since the separation between the peaks with a low $|m|$ falls below the spectral resolution, we select only a number of peaks for the analysis, as shown in Fig. 3 (14 and 18 peaks in spectra 1 and 2, respectively). Within the selected peaks, the spectral separation between the highest wavelength peak ($|m| = h$) and a given peak ($|m| = h + x$) is given according to Eq. (1) as: $\Delta\lambda(h, h+x) = a[(h+x)^2 - h^2]$, where $a = -e\lambda_0/[2l(l+1)]$. Experimentally determined spectral separations between selected peaks are matched with this expression by choosing the integer value of h that leads to the lowest error (see inset of Fig. 3c). The value of h determined in this way is then used to determine the $|m|$ values of all the selected peaks. As shown in Fig. 3c, our calculations fit very well with the experimental data. The linear dependence of $\Delta\lambda$ on $m^2 = (h+x)^2$ is another justification for the deformation towards a prolate spheroid in our experiments [7].

For the spectra 1 and 2 presented in Fig. 3, the lowest wavelength peaks are determined to have $|m|$ values of 31 and 30, respectively. We next compare these values with the expected angular momentum numbers l. At 62±5% relative humidity, the refractive index of the glycerol–water microdroplet is determined to be 1.4210 ± 0.0064 [11]. The l values are found by matching the theoretically expected WGM frequencies with three peaks spanning two free spectral ranges (recorded with a low spectral resolution, data not shown), for each microdroplet. For the high quality WGMs that we study (radial mode number $n = 1$), l values are then determined as 34 and 32 for microdroplets 1 and 2, respectively. The microdroplet radii associated with these values are 2.6 and 2.5 μm.

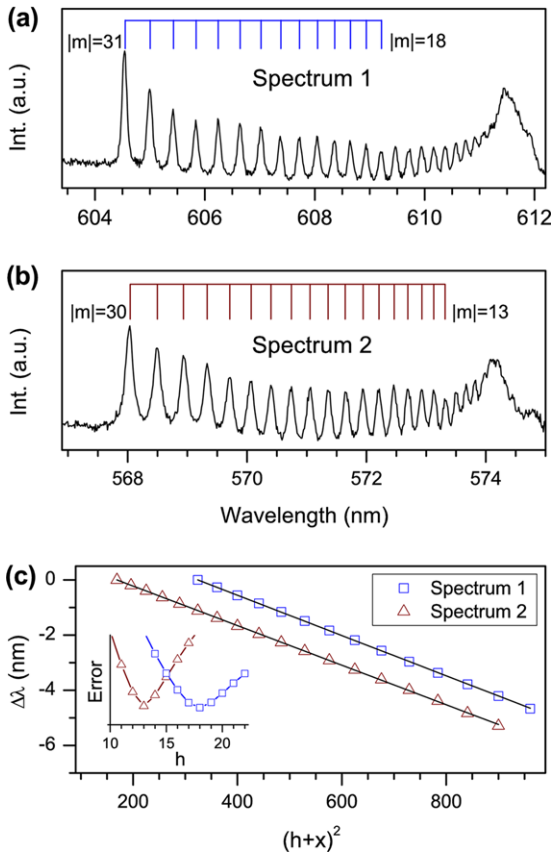

Fig. 3. (a, b) High voltage spectra recorded from microdroplets 1 (a) and 2 (b). Isolated sharp peaks correspond to twofold degenerate WGMs. The well-resolved peaks used in the analyses are indicated. Applied voltages and contact spacings are 350 V, 37 μm and 320 V, 33 μm for spectra 1 and 2, respectively. (c) Measured peak positions are shown as squares (Spectrum 1) and triangles (Spectrum 2). Solid lines indicate the best fit curves. Inset: Error as a function of h obtained by matching the separations between the selected peaks to the theoretical formula.

In the experiments we have consistently observed maximum $|m|$ values to be smaller than the expected l values for at least three other microdroplets. This discrepancy is attributed to the contact with the surface whose high refractive index will prevent the confinement of the WGMs beyond a maximum $|m_{max}|$ value. The approximate formula in reference [8], valid for large l and for $|m| \approx l$, gives the angular distributions of the WGMs with $|m| > |m_{max}|$. An estimation of the contact angle follows with simple geometrical considerations using the angular positions of the intensity maxima of the WGMs. With this method, contact angles are estimated to be $160^\circ < \theta_1 < 164^\circ$ and $164^\circ < \theta_2 < 170^\circ$ for microdroplets 1 and 2, respectively. We note that, in our case, contact angle estimations made for high voltages should also be valid at low voltages due to relatively small deformations, and to the very little concentration of ions in the microdroplets which prevents electrowetting [15]. Our estimations are in agreement with the contact angle measurements performed on millimetric droplets using the specific superhydrophobic surface that we employ [16].

In conclusion, by using a uniform electric field we have demonstrated controlled lifting of the azimuthal degeneracy of the WGMs of glycerol–water microdroplets standing on a superhydrophobic surface. The measured spectral positions of the nondegenerate WGMs fit very well with the deformation of a microdroplet towards a prolate spheroid. Our results revealed fewer azimuthal modes than expected from an ideal sphere. This difference, that is attributed to the truncation due to the contact with the surface, allowed for estimations of the contact angles. Hence, the presented technique can be explored for the development of novel devices that measure the contact angles of microdroplets standing on a superhydrophobic surface. For future studies, salt-water microdroplets kept in a humidity chamber can be employed to achieve more stable experimental conditions and benefit from largely tunable WGMs [17]. Our results can also inspire novel electrically tunable devices for applications in optoelectronics optofluidics. Other fundamental studies on WGMs can also be envisioned especially using different electrical contact geometries.

Acknowledgements

The authors thank the Alexander von Humboldt Foundation for equipment donation, A.F. Coskun for assistance in initial experiments, H.I. Ocakli and M.S. Kilic for help in photolithography, and Seniz Türküz and Hüseyin Parlar for ITO coating. A. Kiraz acknowledges the financial support of TÜBA in the framework of the Young Scientist Award program (Grant No. A.K/TÜBA-GEBIP/2006-19). M. Mestre acknowledges partial supports from TÜBİTAK and the Koç University postdoctoral fellowship program.

References

[1] V.S. Ilchenko, A.B. Matsko, IEEE J. Sel. Topics Quantum Electron. 12 (2006) 15.
[2] R.K. Chang, A.J. Campillo (Eds.), Optical Processes in Microcavities, World Scientific, 1996.
[3] A. Kiraz, A. Kurt, M.A. Dündar, A.L. Demirel, Appl. Phys. Lett. 89 (2006) 081118.

[4] C.F. Bohren, D.R. Huffman, Absorption and Scattering of Light by Small Particles, Wiley-VCH, 1998.
[5] M.I. Mishchenko, A.A. Lacis, Appl. Opt. 42 (2003) 5551.
[6] G. Chen, R.K. Chang, S.C. Hill, P.W. Barber, Opt. Lett. 16 (1991) 1269.
[7] G. Chen, M.M. Mazumder, Y.R. Chemla, A. Serpengüzel, R.K. Chang, S.C. Hill, Opt. Lett. 18 (1993) 1993.
[8] J.C. Knight, N. Dubreuil, V. Sandoghdar, J. Hare, V. Lefevre-Seguin, J.M. Raimond, S. Haroche, Opt. Lett. 20 (1995) 1515.
[9] A.J. Trevitt, P.J. Wearne, E.J. Bieske, M.D. Schuder, Opt. Lett. 31 (2006) 2211.
[10] M. Gerlach, Y.P. Rakovich, Opt. Express 15 (2007) 3597.
[11] A. Kiraz, Y. Karadağ, M. Muradoğlu, Phys. Chem. Chem. Phys. 10 (2008) 6446.
[12] G. Taylor, Proc. Roy. Soc. Lond. A 291 (1966) 159.
[13] S. Torza, R.G. Cox, S.G. Mason, Phil. Trans. R. Soc. A 269 (1971) 295.
[14] D. Khossravi, K.A. Connors, J. Solution Chem. 22 (1993) 321.
[15] A. Kiraz, Y. Karadağ, A.F. Coskun, Appl. Phys. Lett. 92 (2008) 191104.
[16] M.Y. Yüce, A.L. Demirel, F. Menzel, Langmuir 21 (2005) 5073.
[17] A. Kiraz, Y. Karadag, S.C. Yorulmaz, M. Muradoglu, Phys. Chem. Chem. Phys. 11 (2009) 2597.